Available online at www.sciencedirect.com
SCIENCE DIRECT®
Journal of Power Sources 135 (2004) 152–164
JOURNAL OF POWER SOURCES
www.elsevier.com/locate/jpowsour

Experimental evaluation and semi-empirical modeling of *U/I* characteristics and methanol permeation of a direct methanol fuel cell

H. Dohle*, K. Wippermann

Forschungszentrum Jülich GmbH, Institut für Werkstoffe und Verfahren der Energietechnik (IWV3), D-52425 Julich, Germany

Received 28 August 2003; received in revised form 24 February 2004; accepted 22 April 2004

Available online 3 July 2004

Abstract

The operating conditions of a direct methanol fuel cell (DMFC) are important with regard to the power output and the efficiency of the cell. Especially the methanol concentration influences the overpotentials of both the anode and the cathode. Furthermore, the efficiency depends on the amount of methanol losses due to methanol permeation. The goal of this paper is to investigate the anode, the cathode and the methanol permeation of a DMFC experimentally to obtain a set of parameters for a DMFC model. The developed model predicts the *U/I* characteristics as well as the methanol permeation for different operating conditions.

Keywords: DMFC; Model; Methanol permeation; Power; Efficiency

1. Introduction

Direct methanol fuel cells (DMFC) are expected to appear in the market within the next few years especially for portable electronic devices and other applications in the low power range. There, they offer the advantage of easy storage and easy refilling of the liquid methanol. Recently, DMFC stacks and system in the power range from several watts to 2 kW class have been reported [1–3].

As compared to hydrogen driven systems, the system design and the operation of DMFC is much simpler. Although H_2-PEFC and DMFC have nearly the same theoretical open circuit voltage (1.23 V versus 1.21 V) the cell voltage and the power density in DMFCs are lower due to electrochemical losses. At present, catalyst loadings of the DMFC electrodes are substantially higher than those in PEFC. Therefore, a present focus in research is the design of DMFC stacks and membrane electrode assemblies (MEAs) with reduced catalyst loadings. In addition, the knowledge about the processes in the DMFC as anode and cathode overpotentials or methanol permeation is important, as the different processes interact and may affect the power and the efficiency of the stacks [4,5].

In the low temperature range, DMFCs are operated with a liquid water/methanol mixture. The cathode is fed with oxygen or air. In a direct methanol fuel cell, the following catalytically activated reactions take place:

$$\text{anode}: \quad CH_3OH + H_2O \Rightarrow CO_2 + 6H^+ + 6e^-$$

$$\text{cathode}: \quad 6H^+ + 6e^- + 1.5O_2 \Rightarrow 3H_2O$$

$$\text{overall reaction}: \quad CH_3OH + 1.5O_2 \Rightarrow CO_2 + 2H_2O$$

The main problem of the DMFC anode is the multistage nature of the reaction. In DMFCs, CO or COH occurs as stable and adsorbed intermediates of methanol oxidation. These adsorbants lead to considerable high anodic overpotentials lowering the cell voltages significantly below the theoretically expected values. At anodic potentials less than +500 mV versus the reversible hydrogen potential, the oxidation of methanol is initiated by a dehydrogenation reaction of the methanol [6–14]. At higher potentials, methanol oxidation takes place through a reaction with adsorbed oxygen or OH [6–14]. In liquid operated DMFC, the methanol concentration has specific importance with regard to the diffusion overpotentials. Too low a methanol concentration leads to increased diffusion overpotentials. Generally, diffusion overpotentials can be prevented by the use of sufficiently high methanol concentrations. On the other hand, this may cause high methanol permeation rates and, therefore, methanol losses. If the cathode catalyst also promotes the methanol oxidation, the formation of a mixed methanol/oxygen potential lowers the cathode potential.

* Corresponding author. Fax: +49 2461 61 6695.
E-mail address: h.dohle@fz-juelich.de (H. Dohle).

0378-7753/$ – see front matter © 2004 Elsevier B.V. All rights reserved.
doi:10.1016/j.jpowsour.2004.04.014

Nomenclature

a	constant
c	concentration
c_{ref}	reference concentration
d	membrane thickness
d_{ref}	reference membrane thickness
DMFC	direct methanol fuel cell
E	voltage
E_0	open circuit voltage
F	Faraday's constant
$f_{1–4}$	fitting parameters
i	current density
i_*	exchange current density
i_{ion}	ionic current density
I	current
K	constant
l_{mem}	membrane thickness
l_{ca}	thickness of catalyst layer
$m_{1,2}$	fitting parameters
M	molar concentration
MEA	membrane electrode assembly
n_{drag}	electro-osmotic drag factor
PEM	polymer electrolyte membrane
R	molar gas constant
RE_C	Reference Electrode (cathode)
T	temperature
α	transfer coefficient
γ	reaction order
η_{an}	anode overvoltage
η_c	cathode overvoltage
η_{ohm}	ohmic losses
σ_{mem}	membrane conductivity

The goal for the model is to study optimized operating conditions using reliable information about the processes in DMFC as overpotentials or methanol permeation obtained in measurements. In addition, the model can be used to examine possible aspects like membrane materials with different proton conducting behaviour or different methanol permeation properties. In the literature, many models describing the DMFC are present. In [15,16], the main effects in a DMFC are described by mathematical models for the mass transport in the porous electrode structures and the potential and concentration distributions in the electrode regions. There, the voltage loss due to methanol permeation is assumed to be proportional to the methanol permeation. In another mathematical approach [17], special focus is taken on the mass transport of methanol in the gas diffusion layer and the ionic phase to predict the methanol permeation. Furthermore, the mixed potential at the cathode is calculated as a superposition of the methanol oxidation and the oxygen reduction. A macrohomogeneous porous electrode describing the reactions and the transport within the catalyst zone of the methanol electrode is shown in [18]. There, effects of catalyst zone thickness, catalyst loading and polymer electrolyte loading are discussed by the means of a mathematical approach. In [19], an equation is given which is based on a semi-empirical approach. Methanol oxidation and oxygen reduction kinetics are combined with effective mass transport coefficients for the fuel cell electrodes. Reference [20] describes a model particularly for the DMFC anode taking into account non-Tafel kinetics of electrochemical reaction of methanol oxidation, diffusion transport of methanol through the backing layer and methanol permeation where the total limiting current density appears to be a combination of reaction- and diffusion-limiting current densities. Another mathematical model for the anode of a direct methanol fuel cell is presented in [21]. This model considers the mass transport in the whole anode compartment and the proton exchange membrane (PEM), together with the kinetic and ohmic resistance effects through the catalyst layer. Furthermore, the influence of, e.g. catalyst layer parameters on the methanol permeation and anode performance is investigated.

2. Experimental

The following characteristics of DMFC fuel cell have been experimentally determined:

- current versus anode potential,
- cell potential versus current,
- methanol permeation.

For the measurement of the different characteristics, different test rigs were used.

2.1. Test cell for DMFC anode characterization

For the evaluation of DMFC anode, a separate apparatus with a three electrode setup was used [22]. Schematic drawings of the measuring apparatus and the MEA are shown in Fig. 1. All the electrochemical measurements, i.e. quasi-stationary current/potential curves (scan rate: 0.5 mV/s), cyclic voltammograms (scan rate: 20 mV/s) and impedance spectra were performed with a three electrode arrangement. The impedance spectra were used for *IR*-correction and will not be discussed in detail. The electrode potential, U (RE_C), is measured versus the reference potential of the hydrogen reaction established at the ring (and the counter electrode).The anode chamber was always supplied with an aqueous solution of methanol and the cathode chamber was filled with water, which was saturated with hydrogen. All measurements were carried out under ambient pressure. Both liquids were pumped from two thermostated vessels to the electrode chambers and backwards with a rate of 200 ml/min. The temperature was varied from 30 to 70 °C. All the electrodes, which consisted of both a catalyst and a backing layer, were electrically contacted by platinum grids and wires. The Pt grids were pressed onto

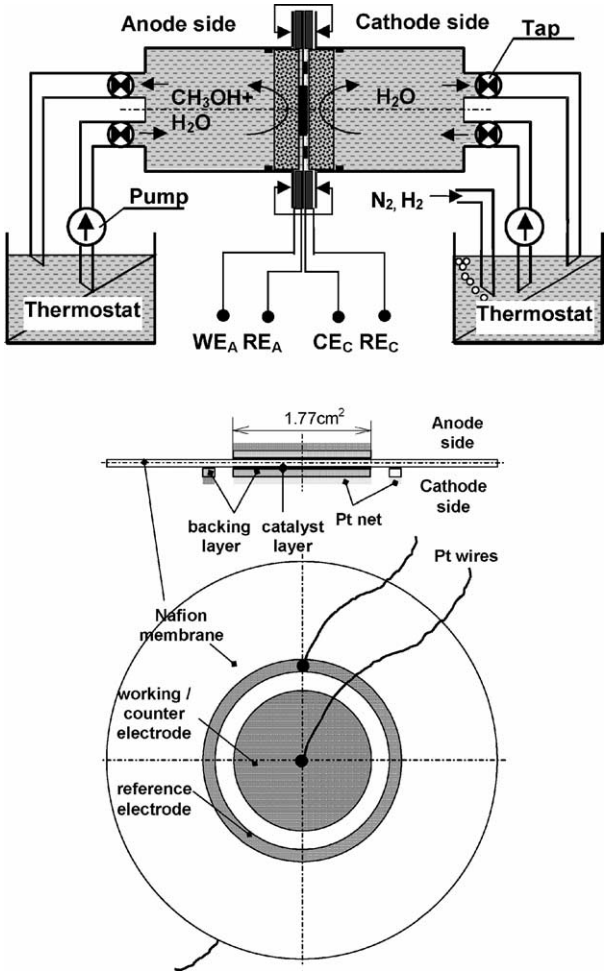

Fig. 1. Three electrode measuring setup for half cell measurements. Top: test equipment. Bottom: three electrode membrane electrode assembly for half cell measurements.

the electrodes by using highly porous filter plates made of glass. The Nafion 117 membrane had a diameter of 80 mm and the electrodes had a diameter of 15 mm corresponding to an electrode area of about 1.8 cm^2. The ring-shaped reference electrode placed on the cathode side of the MEA had an inner diameter of 20 mm and an outer diameter of 26 mm.

2.2. Test cell and test rig for cell characterization

The cells and membrane electrode assemblies were characterized by different test rigs. For the evaluation of current/density characteristics as well as the measurement of the methanol permeation the test cell and the test rig, shown in Figs. 2 and 3, were used [19]. The active area of the MEA is 20 cm^2. Electronic contacting of the MEA as well as the provision of the reaction media is always effected with the aid of a grid structure. The cell consists of titanium. The non-conducting intermediate frame acts on the one hand as an additional electric insulation of anode and cathode and, on the other hand, as a centring aid during installation of the membrane electrode assembly. The inactive rim of the MEA along with two PTFE sealings serves for the gas-tight separation of the anode and cathode compartments.

The test rig consists of an anode loop for the methanol/water mixture with separation and removal of the CO_2 gas bubbles. Any methanol reaching the cathode is converted into CO_2 at least in the catalytic burner placed behind the cathode cell outlet. Then, the amount of CO_2 resp. the methanol permeation is measured by an infrared CO_2 detector (Vaisala GMM 12 A) which is placed in the cathode exhaust gas stream. Depending on the membrane, the catalyst layer structures and the operating conditions the amount of CO_2 which passes from the anode to the cathode must be measured separately. Details of this method are given in [23].

The test rig shown above can be used further for the investigation of the anode potential at elevated pressures and

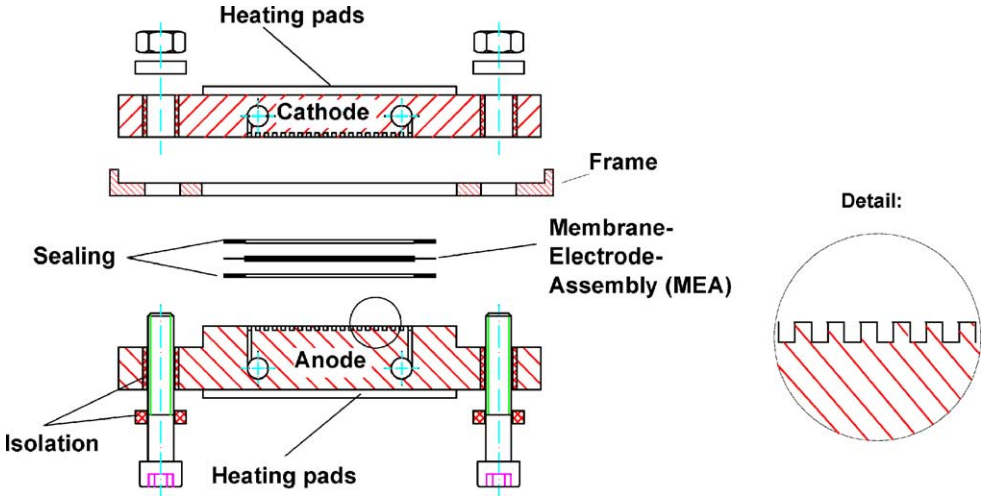

Fig. 2. Test cell for *U/I* characteristics.

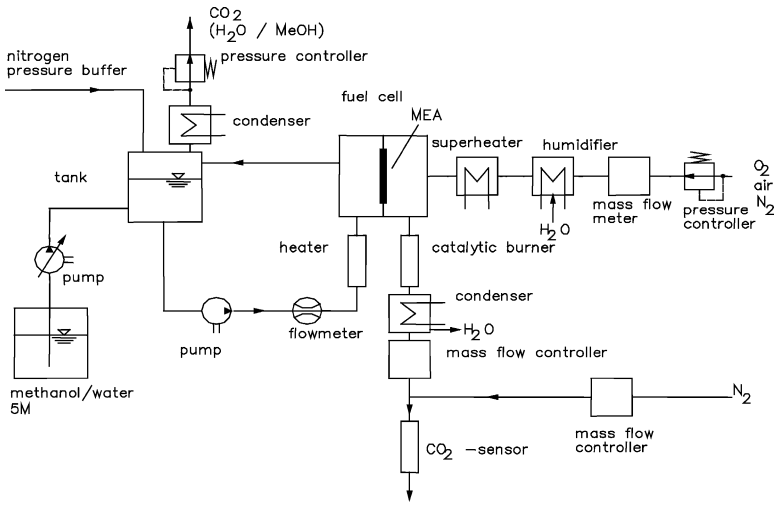

Fig. 3. Schematic of the test rig used for the measurement of methanol permeation and *U/I* characteristics.

temperatures which are not suitable for the test rig specifically designed for anode potential measurements. For these measurements, the cathode chamber is filled with hydrogen. Then, additional hydrogen is produced at the cathode by applying a current through the cell by means of an external current source. The method used is based on the hydrogen production in the cathode chamber of the test cell. This changes the cathode of the fuel cell into a dynamic hydrogen electrode with an overpotential negligible compared to the methanol electrode. As a result, in a first approximation the resulting cell voltage is the sum of ohmic losses in the membrane and the overpotentials in the methanol oxidation electrode. The corresponding ohmic losses were determined by the current interruption technique [24]. At elevated temperatures, the test rig is pressurized to keep the water/methanol mixture liquid.

During the experiments, different types of membrane electrode assemblies have been used to investigate if the model to be developed is suitable for a wide range of operating conditions independent on the different MEA preparation methods. In addition, data taken from literature are used for model evaluation and verification.

2.3. Membrane electrode assembly type A

These MEA was prepared in-house by a spraying method. The anode backing layer consisted of a microlayer composed of uncatalysed XC-72 active carbon (6 mg/cm^2) and 15 wt.% PTFE (Dyneon). The microlayer was supported on a carbon cloth (E-TEK). The anode catalyst layer contained 4 mg/cm^2 of Pt/Ru catalyst (50:50) on carbon XC-72 and 20 wt.% Nafion from a 5% Nafion solution. The cathode was similarly constructed with 4 mg/cm^2 of Pt black with 10% Nafion. The backing layer was composed of a hydrophobized carbon cloth (E-TEK, 8 mg/cm^2) and a 8 mg/cm^2 microlayer consisting of XC-72 and 40 wt.% PTFE. The MEA was fabricated by hot pressing both electrodes with a Nafion 117 membrane at 130 °C.

2.4. Membrane electrode assembly type B

The membrane electrode assemblies type B are used for half cell measurements. The anode catalyst layers were prepared by spraying a mixture of unsupported Pt/Ru (1:1) black (Johnson Matthey), an appropriate amount of 5% Nafion solution (Aldrich) and isopropanol onto a backing layer made of 87 wt.% carbon black (XC-72) and 13 wt.% PTFE supported by carbon cloth (E-Tek, Inc., 'A' cloth). The catalyst loading was 1.9 mg/cm^2. The anodes were hot pressed ($T = 130$ °C) onto Nafion 117 membranes and acted as working electrodes. Pt black catalyst layers with 9 wt.% Nafion were used as counter and reference electrodes.

2.5. Cell voltage

An example of *U/I* characteristics of a DMFC is shown in Fig. 4. High methanol concentrations prevent the anode from the formation of significant overpotentials. The maximum current density achievable with a 0.25 M concentration is 200 mA/cm^2. Doubling the concentration to 0.5 M doubles the limiting current. On the other hand, attention must be paid on the methanol permeation which—for a given temperature—depends on the current density as well as on the concentration. Using a 2 M methanol concentration lowers the cell voltages compared to the 1 M concentration which is caused by the impact of the methanol permeation on the cathode potential. Therefore, the optimum methanol concentration depends on the current density. In the low current regime, ($i < 100$ mA/cm^2) the 0.25 M concentration is best, whereas at higher currents, (100 mA/cm^2 $< i <$ 250 mA/cm^2), use of a 0.5 M methanol solution is accompanied with the highest power output.If the current density

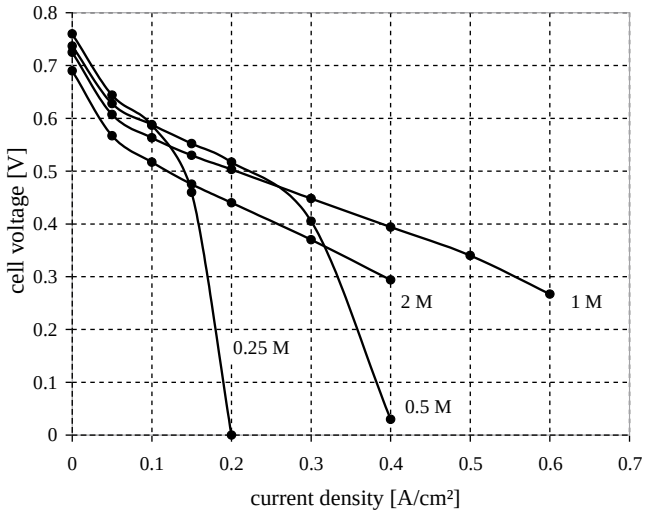

Fig. 4. *U/I* characteristics of a DMFC at different methanol concentrations; operating conditions: 110 °C, cathode and anode pressure 3 bars, oxidant O_2.

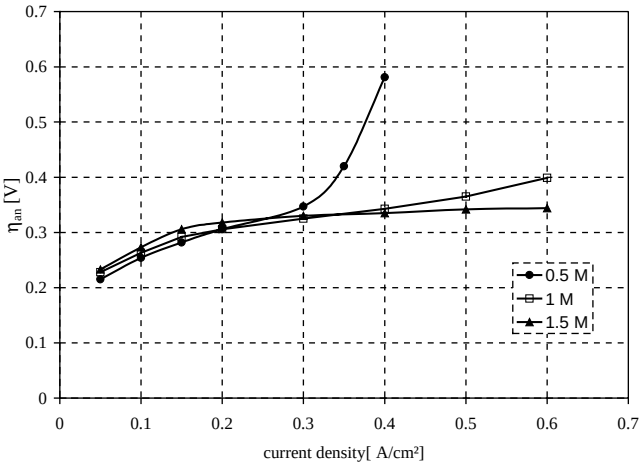

Fig. 5. Anode potential as a function of concentration at 110 °C; cathode and anode pressure 3 bars; MEA type A.

is further increased, the optimum methanol concentration is 1 M.

In order to distinguish the different influences of the methanol concentration on the anode and the cathode, the anode overpotential and the methanol permeation were determined separately.

The anode overpotential/current characteristics at 110 °C and different methanol concentrations are given in Fig. 5. With a methanol concentration of 0.5 M, a limiting current of about 400 mA/cm^2 can be observed leading to a significantly increase in the anodic overpotential 600 mV which is approximately 270 mV higher than the corresponding anodic overpotential for a methanol concentration of 1 M. This is in agreement with the behaviour of the whole cell (see Fig. 4). According to Kauranen et al. [14], the limiting current of methanol oxidation on platinum ruthenium can predominantly be attributed to a saturation of the coverage by hydroxyl groups on the catalyst surface. However, permeation experiments prove, that also mass transport limitations, i.e. the diffusion of methanol plays an important role (see below).

In 1 and 1.5 M methanol solution, the limiting current is much higher than the maximum current density investigated. Furthermore, in case of the 1.5 M methanol solution, no reaction or diffusion overpotential is observed.

Finally, the methanol permeation for the given operating conditions is shown in Fig. 6. Three different methanol concentrations (0.5, 1 and 1.5 M) have been tested. The measurements include corrections for the CO_2 passing from the anode to the cathode and are detected additionally in the previously described CO_2-sensor. Without CO_2-correction,

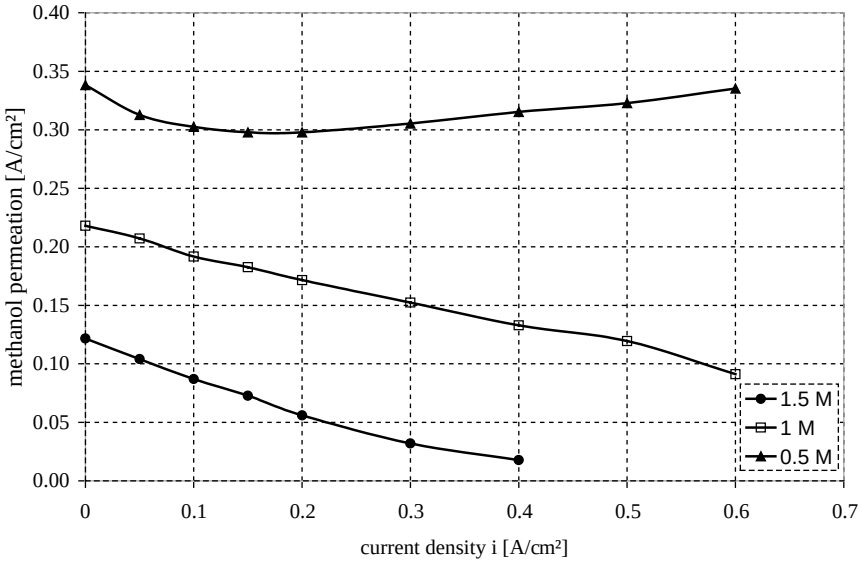

Fig. 6. Methanol permeation as a function of methanol concentration and current density.

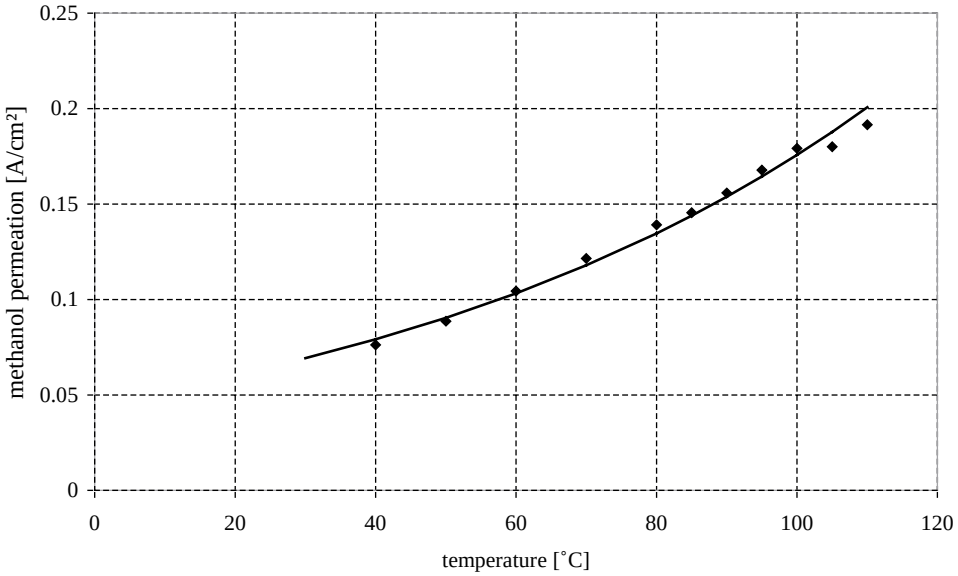

Fig. 7. Methanol permeation as a function of temperature. Current density $i = 0$. MEA type A.

the measured methanol permeation is too high especially at high current densities. Details of the method are given in [23]. Using the lowest methanol concentration of 0.25 M the methanol permeation decreases to approximately 20 mA/cm^2 at a current density of 400 mA/cm^2 indicating a depletion of methanol in the interface between anode catalyst layer and membrane. This is in good agreement with the observed limiting current behaviour at the same current density.

Furthermore, the methanol permeation as a function of temperature is given in Fig. 7 for the open circuit condition. Increasing the temperature, e.g. from 60 to 110 °C doubles the methanol permeation. This is mainly due to increased diffusivity of methanol in the water and the membrane. With rising current densities, the electro-osmotic drag becomes predominant compared to the diffusion. The drag coefficient n_{drag}, describing the ratio of transported molecules to transporting protons, is temperature dependent as well e.g. $n_{drag} = 2$ at 15 °C reaching 5.1 at 130 °C [25].

To investigate the influence of the temperature on the anode overpotential characteristics, measurements in the test cell with three-electrode MEAs were performed. The results of these measurements are shown in Fig. 8.

3. Model development

The new model is based on the experiments presented above with the processes schematically shown in Fig. 9. The goal of this model is to predict the main processes as

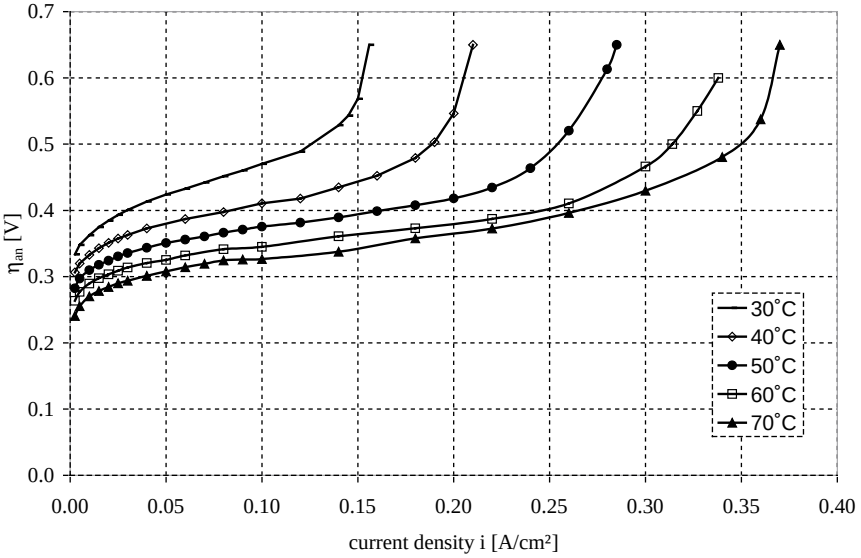

Fig. 8. *IR*-corrected anode polarization curves as a function of temperature at 1 M methanol concentration. MEA type B.

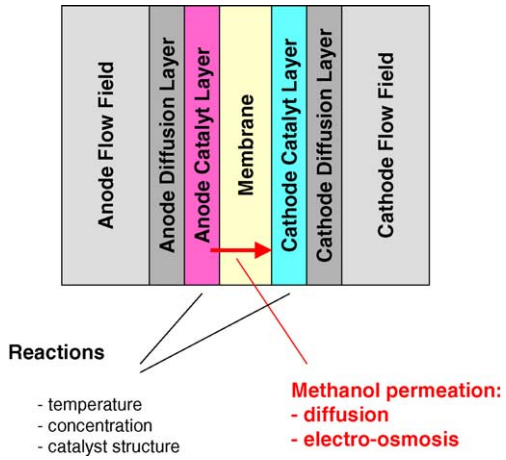

Fig. 9. Schematic of a direct methanol fuel cell.

methanol permeation and overpotentials resulting in specific current/voltage characteristics in a wide range of operating conditions. In a future step, the model will be used to predict the power and efficiency of a DMFC system as a function of its operation conditions. For reasons of clarity and usability the model should be simplified to contain as few parameters as possible.

The cell voltage of a DMFC is calculated by the theoretical open voltage less the overpotentials η_{an}, η_c and the ohmic losses η_{ohm}.

$$E = E_0 - \eta_{an} - \eta_c - \eta_{ohm} \quad (1)$$

The theoretical open circuit voltage E_0 can be calculated using Nernst's equation. Its value is $E_0 = 1.21\,V$ for standard conditions.

3.1. Physical model of the anode overpotential

The anodic overpotential is mainly a function of the reaction rate, the methanol concentration and the temperature. Eq. (2) given by Meyers and Newman [26] is a simplification of the four step mechanism proposed by Gasteiger et. al in [11] resulting in a simplified two step mechanism. The first step is adsorption of methanol and ionization of adsorbed species followed by a second step containing the associative ionization of adsorbed CO with water molecules.

$$i = \frac{i_* c_M a \exp(2.303\eta/b)}{c_M + Ka\exp(2.303\eta/b)} \quad (2)$$

with i_* as the exchange current density of the anode [A/cm^2], c_M the methanol concentration in the catalyst layer, b represents the Tafel slope, K and a are constants.

For large methanol concentrations c_M and small overpotentials η Eq. (2) describes zero-order kinetics. In this case, the exponent in the denominator can be neglected with the result that the current i is independent of the methanol concentration and is a function only of the overpotential.

$$i = i_* a \exp\left(\frac{2.303\eta}{b}\right)$$

for large methanol concentrations and small η (3)

In contrast, for high overpotentials, η, the concentration term in the denominator can be neglected indicating a transition to first-order kinetics. Then, the current is limited by the finite rate of methanol adsorption on the catalyst layer which is proportional to the methanol concentration.

$$i_{lim} = \frac{i_* c_M}{K} \quad \text{limiting current for high } \eta \quad (4)$$

In the following, both the physical model and the semi-empirical model are fitted to the experimentally observed data. The fitting parameters are summarized in Table 1.

3.2. Semi-empirical equation

The anode overpotential is fitted by the following semi-empirical equation:

$$\eta_{an} = f_1 + f_2\ln(i) + f_3\exp\left(\frac{f_4 i}{c_M}\right) \quad [V] \quad (5)$$

This equation delivers the overvoltage directly as a function of the current density which is beneficial for numerical implimentation to calculate Eq. (1), whereas the equation of Meyers and Newman cannot be transformed to give η_{an} as a function of the current density i.

Table 1
Fitting parameters for the polarization curves of the MEA anodes shown in Fig. 10

Anode fitting parameters for								
Concentration (M)	The semi-empirical equation[a]				Meyers and Newman[b]			
	f_1 (V)	f_2 (V)	f_3 (V)	f_4 (mol/l)/(A/cm^2)	I_* (A/cm^2)	a [−]	b (V)	K (M)
MEA type A 110 °C, 3 bars								
0.5–1.5	0.3949	0.0603	4.3565E-5	10.81	1.22E-4	0.2	0.074	1.6E-4
MEA described in literature [14]								
0.02–0.5	0.594	0.0369	4.3565E-5	8.4	5.11E-7	0.2	0.085	4.955E-7

[a] $\eta_a = f_1 + f_2\ln(i) + f_3\exp\frac{f_4 i}{c_M}$.
[b] $i = \frac{i_* c_M a\exp(2.303\eta/b)}{c_M + Ka\exp(2.303\eta/b)}$.

In general, this equation is a combination of Tafel-kinetics with an additional exponential term describing the formation of limiting current behaviour.

The constant f_1 and the logarithmic expression of Eq. (5) can be derived partially from Eq. (2), respectively Eq. (3) for the case of small overpotentials and large methanol concentrations. Then, they contain the tafel slope b as well as the exchange current density i_*. The logarithmic term dominates in the regime of low current densities.

Of course, alternatively these parameters can be obtained by simple fit procedures on the basis of the experimental data. This alternative approach is necessary if the first approach by Meyers and Newman does not give sets of parameters which fit the experimental data. Comparing the coefficients in Eq. (3) and Eq. (5) leads to the following analogy:

$$[\mathrm{V}] \quad f_1 = \frac{b}{2.303}, \qquad [\mathrm{V}] \quad f_2 = \frac{b}{2.303} \ln \frac{\mathrm{A/cm^2}}{ai^*} \tag{6}$$

The last term of the sum in Eq. (5) finally increases the overpotential η_{an} with increasing current density. It can be easily seen that higher methanol concentrations shift the begin of limiting current behaviour towards higher current densities.

A similar expression is described in [27] for the cathodic overpotential of a PEM with the exponential-term for fitting the limiting current behaviour due to oxygen depletion. Analogously, the exponential-term is used in our DMFC modeling to describe the increase of the anode overpotential at too low methanol concentrations.

As experimentally observed, the anode overpotential of a DMFC follows typical curves with characteristics as asymptotes, ranges with semi-linear behaviour, inflection points and offset to the hydrogen reversible potential. For a given DMFC anode, these characteristic points mainly depend on the temperature and the methanol concentration.

Fig. 10 shows experimental data and fitting curves for an in-house prepared MEA (left) and for data taken from the literature (right, [14]). The fitting parameters are summarized in Table 1. For each MEA investigated, the parameter f_4 is reciprocal to the concentration, i.e. the impact of diffusion and reaction overpotentials is linearly coupled to the methanol concentration if the temperature is maintained. Of course, changing the temperature influences the beginning of limiting current behaviour as increasing temperature increases the diffusion coefficient.

To investigate the influence of the temperature on the current/density characteristics, the measurements described above with constant methanol concentration and temperatures varying in the range 30–70 °C were analysed and fitted. As shown in Fig. 11, the potential/current curve shifts nearly parallel towards lower overpotentials if the temperature increases. This is due to increased kinetics and decreased activation overpotential of the methanol oxidation. Furthermore, the beginning of the limiting current behaviour is shifted to higher current densities. The fitting parameters regarding the temperature variation are summarized in Table 2. Although different, but similar, MEAs were investigated the fitting parameters f_1 and f_4 show a clear trend concerning the temperature which can be used in the simulation studies. In the temperature between 3 and 110 °C, the parameter f_1 describing the offset depends linearly on the temperature whereas the parameter f_2 shows Arrhenius behaviour (Fig. 12).

The corresponding fitting equations are:

$$f_1 = -0.0021 \left(\frac{T - 273.15K}{K} \right) + 0.6132 \tag{7}$$

$$f_4 = 0.0297 \exp \left(\frac{2261.7}{T} \right) \tag{8}$$

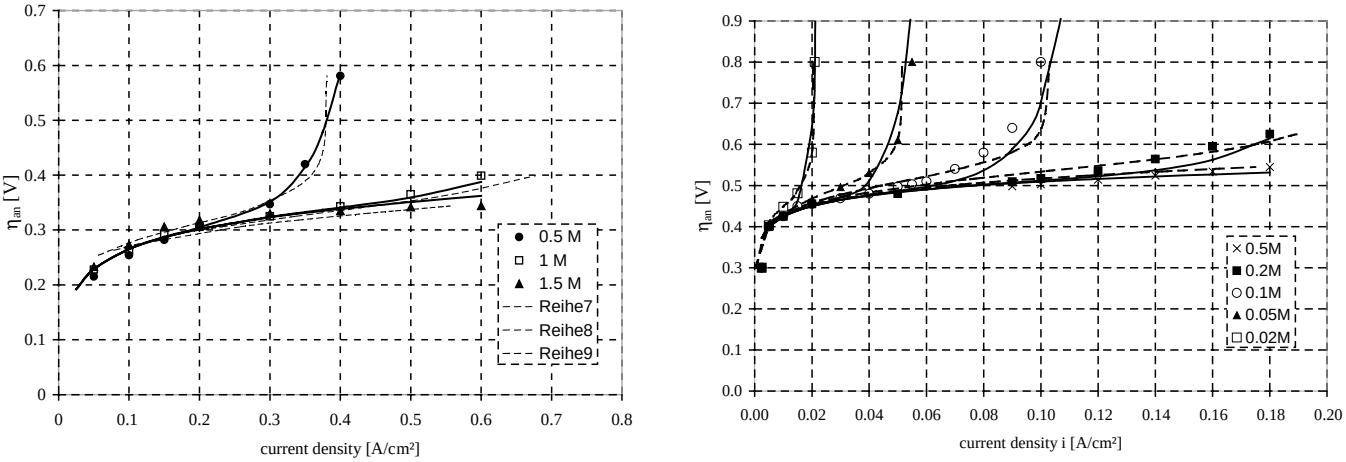

Fig. 10. *IR*-corrected polarization curves of different DMFC anodes as a function of methanol concentration (dots: experimental data, solid lines: fit by the semi-empirical equation, dashed lines: fit by the equation of Meyers and Newman). Left: MEA type A at higher methanol concentrations. Operating conditions: temperature 110 °C, pressure 3 bars, high overstoichiometric flow of methanol. Right: experimental data (dots) taken from Kauranen et al. [14] at 60 °C in 1M H_2SO_4, catalyst loading 7.9 mg/cm^2 Pt/C, ambient pressure.

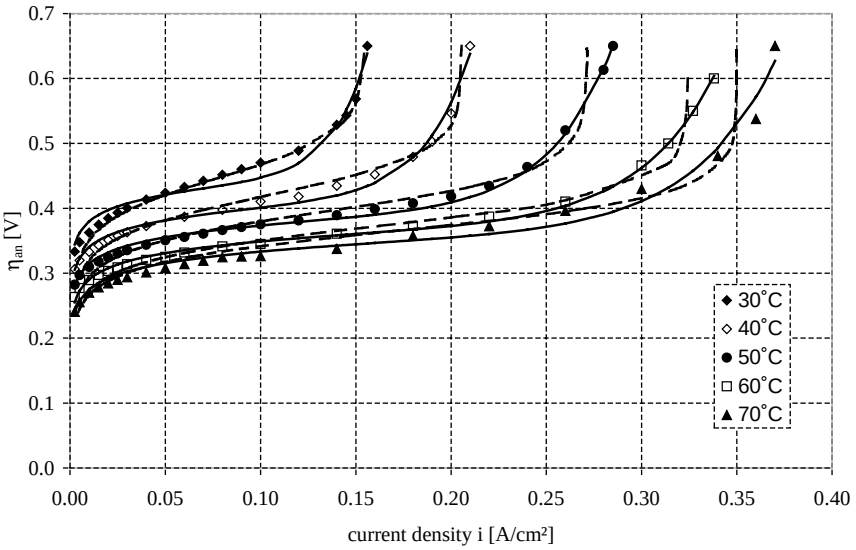

Fig. 11. *IR*-corrected polarization curves as a function of temperature, DMFC MEA type B; dots: experimental data, solid lines: fit by the semi-empirical equation, dashed lines: fit by the equation of Meyers and Newman.

Table 2
Fitting parameters for different temperatures at 1 M methanol solution

Temperature (°C)	Anode fitting parameters for the semi-empirical equation[a]				Anode fitting parameters for Meyers–Newman[b]			
	f_1 (V)	f_2 (V)	f_3 (V)	f_4 (mol/l)/(A/cm^2)	i_* (A/cm^2)	a [−]	b (V)	K (M)
MEA type B 1 M, ambient pressure								
30	0.5679	0.05525	4.3565E-5	53.69	3.97E-6	0.2	0.0850	2.15E-8
40	0.5286	0.05525	4.3565E-5	40.62	4.95E-6	0.2	0.0795	1.90E-9
50	0.5027	0.05525	4.3565E-5	30.41	5.96E-6	0.2	0.0748	1.60E-8
60	0.4785	0.05525	4.3565E-5	25.29	6.96E-6	0.2	0.0705	1.45E-8
70	0.4629	0.05525	4.3565E-5	23.51	7.0E-6	0.2	0.0690	1.30E-8
MEA type A 1 M, 3 bars								
110	0.3949	0.0603	4.3565E-5	10.81	1.22E-4	0.2	0.074	1.6E-4

[a] $\eta_a = f_1 + f_2 \ln(i) + f_3 \exp\frac{f_4 i}{C_M}$.
[b] $i = \frac{i_* c_M a \exp(2.303\eta/b)}{c_M + Ka \exp(2.303\eta/b)}$.

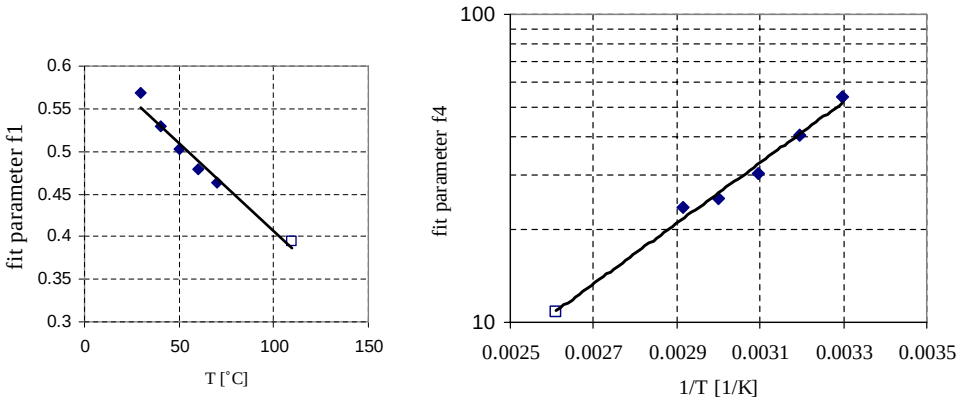

Fig. 12. Influence of the temperature on the fit parameters f_1 and f_4 of the semi-empirical equation for two different MEAs. MEA type A (□); MEA type B (◆).

The parameters f_2 and f_3 do not depend on the temperature. For a given MEA, these values can be set constant for all operating conditions.

3.3. Evaluation of the two different anode fitting approaches

Comparing the two modeling approaches—the semi-empirical approach and the equation of Meyers and Newman—it can be seen that both approaches are in general suitable for modeling the typical characteristics of the experimentally determined anode overpotential. In particular, both approaches include the limiting current behaviour as a function of the methanol concentration and the Tafel-like kinetics at low overpotentials. With regard to the congruence of experimental data and fittig curves, the equation of Meyers and Newman fits best for low concentrations and low temperatures. On the other hand, for higher temperatures (>50 °C) it predicts too abrupt limiting current behaviour. As DMFC are operated at elevated temperatures to obtain high power densities, we have chosen the semi-empirical approach.

3.4. Modeling the methanol permeation

For a calculation of the cathode potential, the methanol permeation must be taken into account. The methanol permeation is the sum of a diffusive and a convective (electro-osmotic) fraction. In the following, the absence of a pressure gradient between anode and cathode is assumed. For given operating conditions as temperature and pressure, the local methanol permeation is assumed to be a linear function of the local current density with an offset m_1 and the slope m_2.

$$i_{\text{perm}} = m_1 + m_2 i \tag{9}$$

The semi-empirical expression Eq. (9) is a result of different influences. At first, the anode catalyst layer represents a sink for methanol and at second, the methanol/water mixture at the boundary between anode catalyst layer and membrane is transported not only by diffusion but also by electro-osmosis to the cathode. Therefore, with increasing current density, the methanol concentration in the boundary between catalyst layer and membrane decreases with the result that both the concentration gradients between anode and cathode decrease as well. Consequently, a decrease in methanol permeation should be expected for increasing current densities.

But, on the other hand, increasing the current density leads to an increase of the methanol transport by electro-osmotic drag. In certain conditions, the consumption of methanol in the anode catalyst layer can be overcompensated by the electro-osmotic transport. Experiments show that at low concentrations e.g. below 2 M at 60 °C, the slope is negative, i.e. the methanol permeation decreases with increasing current density due to the methanol consumption in the catalyst layer. At concentrations above 2 M, the methanol permeation increases as well because the anode catalyst layer has a limited capacity towards methanol oxidation which can be exceeded with increasing concentration. Consequently, the slope m_2 decreases with increasing drag coefficient.

The offset m_1 describes the methanol permeation at open circuit conditions. It mainly depends on the methanol concentration gradient between anode and cathode which is maintained by the continuous oxidation of methanol at the cathode. For reasons of simplification, the concentration is assumed to be proportional to the thickness of the membrane without taking concentration gradients e.g. in the diffusion layers into account. As the concentration gradient in the diffusion layer is known to be nearly negligible [15,16,20,28] the error made by this assumption is reasonable small.

$$m_1 = 4.65E - 2\frac{d}{d_{\text{ref}}}\frac{c}{1\text{M}}\exp(0.01329(T - 273.15K))\frac{\text{A}}{\text{cm}^2} \tag{10}$$

The thickness d_{ref} is the reference thickness of the Nafion 117 membrane used in the experiments (thikness 175 μm).

The drag coefficient n_{drag} is important for the slope m_2. It describes the transport of molecules by the movement of the ions towards the cathode.

$$N^{\text{drag}}_{\text{H}_2\text{O+MeOH}} = n_{\text{drag}}\frac{i_{\text{ion}}}{F} \tag{11}$$

The slope m_2 represents the influence of the current density on the methanol permeation and summarizes effects by methanol consumption in the anode and methanol transport by electro-osmosis. It is a function of the methanol concentration and the drag coefficient n_{drag}. For $m_2 < 0$ the methanol permeation decreases with increasing current density. Finally, $m_2 = 0$ indicates a constant methanol permeation for all current densities. If the methanol concentration is substantially high e.g. higher than 2 M, the methanol permeation increases with increasing current density. Accordingly, high drag coefficients n_{drag} have the same impact as high methanol concentrations, i.e. high drag coefficients lead to increasing methanol permeation. For the most commonly used membrane materials like Nafion and concentrations in the range of 1 M, the slope is negative, i.e. increasing current density lowers the methanol permeation.

Based on these facts, the following semi-empirical expression is assumed for m_2:

$$m_2 = -0.4 + 0.27\frac{n_{\text{drag}}}{n^{\text{ref}}_{\text{drag}}}\frac{c}{c_{\text{ref}}} \tag{12}$$

The value n_{drag} specifies the number of entrained molecules per proton. The drag coefficient as function of temperature was measured with different experimental setups [25,29], and is in the range of $2\,H_2O/H^+$ at 15 °C–$5.1\,H_2O/H^+$ at 130 °C for Nafion. Using the results in [25] the linearized expression for the temperature

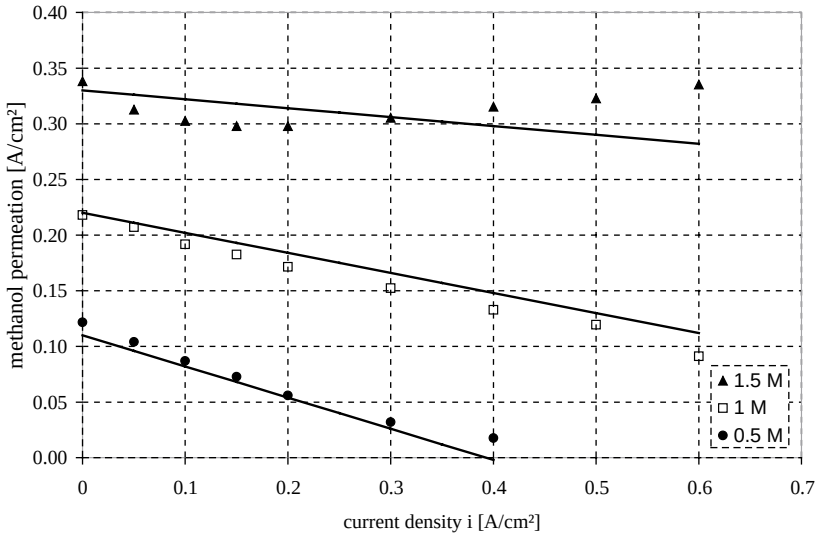

Fig. 13. Fit function (solid line) for the measured methanol permeation (dots) in dependence of the current density at different methanol concentrations.

dependency is

$$n_{\text{drag}} = 4 + \frac{3.1}{115K}(T - 363K) \tag{13}$$

Fig. 13 shows the methanol permeation at different methanol concentrations. With regard to the 0.5 and 1 M concentrations, the fit is reliable. For the highest methanol concentration, 1.5 M, the fit slightly underestimates the increase of methanol permeation at higher current densities. For the practical evaluation of fuel cell operating conditions this error is not relevant as the concentration 1.5 M will not be adjusted for practical use as it is accompanied by too high methanol losses.

3.5. Cathode overpotential

The potential of the cathode is influenced by the methanol permeation, the temperature as well as the current density. The expression for the current density i for the oxygen electrode without permeation is derived from Tafel equation

$$i = l_{\text{cat}} i_* \left(\frac{c_{\text{O}_2}}{c_{\text{O}_2,\text{ref}}}\right)^{\gamma} \exp\left(\frac{\alpha F}{RT}\eta_{\text{c}}\right) \tag{14}$$

with l_{cat} being the catalyst layer thickness, i_* the exchange current density, c_{O_2} the oxygen molar concentration, $c_{\text{O}_2}^{\text{ref}}$ the reference oxygen molar concentration which is a parameter of the given reaction and given catalyst, γ the reaction order (assumed to be 1), η_{k} the overpotential and α being the transfer coefficient [20,27]. An important assumption of Eq. (14) is that the catalyst layer is thin enough to ensure constant reaction rate, oxygen concentration and overpotential. Eq. (14) allows to express the overpotential η_{c} by i:

$$\eta_{\text{c}} = \frac{RT}{\alpha F}\ln\left[\frac{i}{l_{\text{cat}} i_*}\left(\frac{c_{\text{O}_2,\text{ref}}}{c_{\text{O}_2}}\right)^{\gamma}\right] \tag{15}$$

Table 3
Fitting parameters of Eq. (17) for the *U/I* characteristics shown in Fig. 14, simulating a DMFC at 3 bars oxygen and 110 °C

Cathode fitting parameter	Numerical expression
$\frac{RT}{\alpha F}\ln\left[\frac{\text{A/cm}^2}{l_{\text{cat}} i_*}\right]$	0.343 V(0.380 V at 85 °C)
$\frac{RT}{\alpha F}\ln\left[\frac{i}{\text{A/cm}^2}\left(\frac{c_{\text{O}_2,\text{ref}}}{c_{\text{O}_2}}\right)^{\gamma}\right]$	$0.006\ln\left[\frac{i}{\text{A/cm}^2}\left(\frac{1}{3}\right)^{1}\right]$ V
$k(i)$	$\left(0.15\,\text{V} + \frac{0.5\,\text{V}}{\text{A/cm}^2} i\right)\left[\frac{\text{V}}{\text{A/cm}^2}\right]$

For reasons of simplification, the methanol permeation is regarded as an additional impact which increases the cathode overpotential resulting in:

$$\eta_{\text{c}} = \frac{RT}{\alpha F}\ln\left[\frac{i}{l_{\text{cat}} i_*}\left(\frac{c_{\text{O}_2,\text{ref}}}{c_{\text{O}_2}}\right)^{\gamma}\right] + k(i) i_{\text{perm}} \tag{16}$$

respectively

$$\eta_{\text{c}} = \frac{RT}{\alpha F}\ln\left[\frac{\text{A/cm}^2}{l_{\text{cat}} i_*}\right] + \frac{RT}{\alpha F}\ln\left[\frac{i}{A/\text{cm}^2}\left(\frac{c_{\text{O}_2,\text{ref}}}{c_{\text{O}_2}}\right)^{\gamma}\right] + k(i) i_{\text{perm}} \tag{17}$$

with k as an empirical additional factor which considers the impact of methanol permeation in comparison to the impact of the current density i on the cathode potential. An important observation in our modeling studies is that the impact of methanol permeation increases with increasing current density. As a result, the factor k itself depends on the current density. The factor k was determined experimentally by fitting the experimental data in Fig. 4 resulting in the empiric linear expression for k given in Table 3. For the given set of *U/I* characteristics at different methanol concentrations k starts at a relatively low value of 0.15 V per A/cm^2 methanol permeation rate. Increasing the electrical current increases

k to e.g. 0.4 V per mA/cm^2 methanol permeation rate at an electrical current density of 0.5 A/cm^2. For different temperatures, the exchange current density i_* changes as well:

$$i_*(T) = i_*^{\text{ref}} \exp\left[6000\left(\frac{1}{T_{\text{ref}}} - \frac{1}{T}\right)\right] \quad (18)$$

Increasing the temperature from 85 to 110 °C, it tripples the exchange current density which is a reasonable value for this temperature regime. It corresponds to an activation energy of 50 kJ/mol. Detailed data for the activation energy in DMFC-cathodes are given in [30]. For reasons of simplification, the other parameters given in Eq. (17) are set constant, in particular the temperature influence of the methanol permeation on the cathode overpotential is not yet considered due to the lack of experimental data.

Finally, ohmic losses are mainly caused by the membrane resistance. For reasons of simplification, other ohmic losses as losses in the gas diffusion layers and contact resistances are not taken into account. The losses in the membrane are proportional to the thickness l_{mem}.

$$\eta_{\text{ohm}} = \frac{l_{\text{mem}}}{\sigma_{\text{mem}}} i \quad (19)$$

The thickness of the Nafion 117 membrane is 175 μm with a bulk conductivity of 0.1 S/cm.

3.6. Model verification for U/I characteristics

The cathode fitting parameters are given in Table 3. Using Eq. (18) it can be seen that the cathode exchange current density at 85 °C decreases to a third compared to 110 °C. To evaluate the model, the experimentally obtained *U/I* characteristics and methanol permeation rates are compared to the simulated data. Fig. 14 compares the experimental data with the simulated data for a DMFC at 110 °C and 3 bars operating pressure with different methanol concentrations. Above current densities of 30 mA/cm^2, the fit is reliable. The effect of methanol permeation is predicted correctly. Increasing the methanol concentration from 1 to 2 M at 400 mA/cm^2 lowers the cell voltage from 400 to 300 mV. At 50 mA/cm^2, the cell voltage decreases only by 50 mV using 2 M instead of 1 M methanol solution.

Finally, the influence of the temperature on the cell voltage characteristics is shown in Fig. 15. The current/voltage characteristics for 85 °C has been measured at a methanol concentration of 1 M. The temperature dependent fit parameters, f_1 and f_4, for the anode have been derived from the temper-

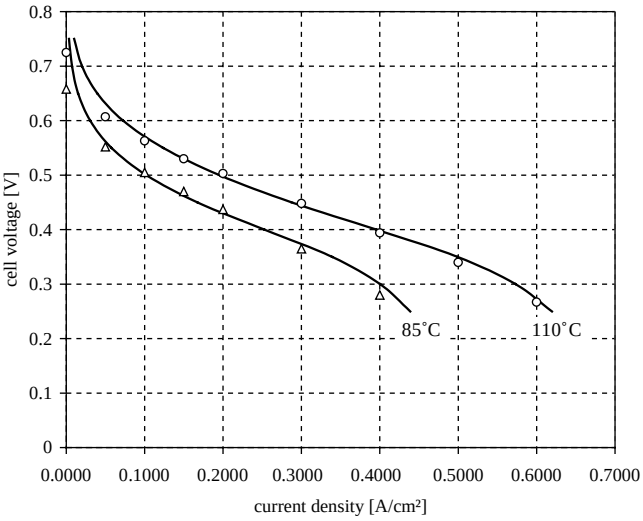

Fig. 15. *U/I* characteristics of a DMFC single cell for a temperature variation. Experimental data: dots, fit: lines. MEA type A, anode and cathode pressure 3 bars.

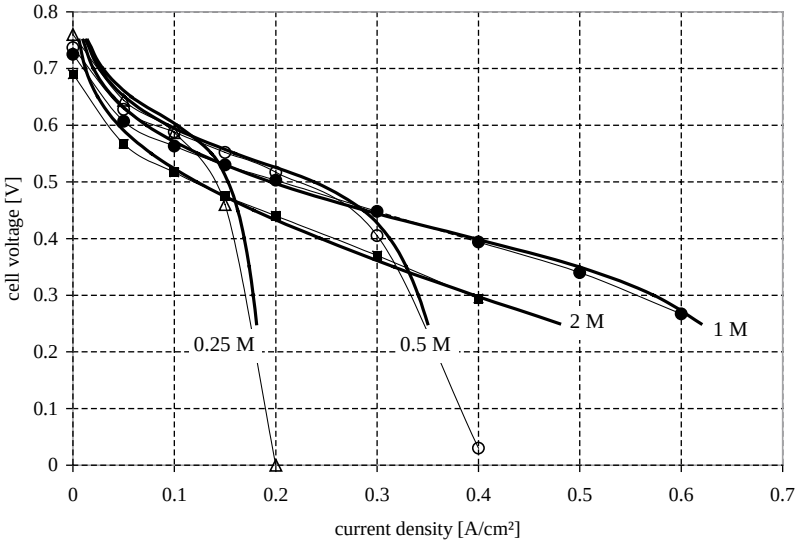

Fig. 14. *U/I* characteristics of a DMFC single cell. Experimental data: dots with thin lines, fit: thick lines. The fit is reliable for current densities >30 mA/cm^2. Fit parameters are: 110 °C, MEA type A, anode and cathode pressure 3 bars, anode set of parameters according to Table 1, cathode fitting parameters according to Table 3.

ature dependency given in Eq. (7) and Eq. (8) Their values at 85 °C are $f_1 = 0.4347$ V, $f_4 = 16.4$ (mol/l)/(A/cm^2), the parameters f_2 and f_3 are unchanged.

4. Conclusions

A simulation model has been developed to predict the current/density characteristics of a DMFC for a wide range of operating conditions. This model is based on several separate experiments for the evaluation of the anode and cathode overpotentials, the methanol permeation and the *U/I* characteristics to obtain a broad set of data describing the characteristics of the single parts of the membrane electrode assembly. The methanol permeation has a substantial impact on the current density and the efficiency. With regard to the methanol permeation the model predicts the impact of the mixed potential at the cathode lowering the *U/I* characteristics of the DMFC. This impact is taken into account by an empirical factor which has been found to increase with increasing current density.

In further studies, this model will be used to determine the influence of design parameters as membrane thickness, drag factor or electrical conductivity on the performance of DMFC.

References

[1] H. Dohle, H. Schmitz, T. Bewer, J. Mergel, D. Stolten, J. Power Sources 106 (2002) 313.
[2] A. Kindler, T.I. Valdez, C. Cropely, S. Stone, Electrochem. Soc. Proc. 4 (2001) 231.
[3] X. Ren, P. Zelenay, S. Thomas, J. Davey, S. Gottesfeld, J. Power Sources 86 (2000) 111.
[4] R.M. Moore, S. Gottesfeld, P. Zelenay, in: Proceedings of the second International Symposium on Proton Conducting Membrane Fuel Cells II, vol. 98-27, p. 388.
[5] H. Dohle, J. Mergel, D. Stolten, J. Power Sources 111 (2002) 268.
[6] V.S. Bagotzky, Y.B. Vasilyev, Electrochim. Acta 9 (1964) 869.
[7] V.S. Bagotzky, Y.B. Vassilyev, Electrochim. Acta 11 (1966) 1439.
[8] V.S. Bagotzky, Y.B. Vassilyev, Electrochim. Acta 12 (1967) 1323.
[9] J.-M. Leger, C. Lamy, Ber. Bunsenges. Phys. Chem. 94 (1990) 1021.
[10] C. Lamy, J.-M. Leger, J. Phys. Chem. 88 (1991) 1649.
[11] H.A. Gasteiger, N. Markovic, P.N. Ross Jr., E.J. Cairns, J. Phys. Chem. 97 (1993) 12020.
[12] H.A. Gasteiger, N. Markovic, P.N. Ross Jr., E.J. Cairns, J. Phys. Chem. 98 (1994) 617.
[13] J.O'M. Bockris, S.U.M. Khan, Surface Electrochemistry: A Molecular Level Approach, Plenum Press, New York, 1993.
[14] P.S. Kauranen, E. Skou, J. Munk, J. Electroanal. Chem. 404 (1996) 1.
[15] K. Scott, W. Taama, J. Cruickshank, J. Power Sources 65 (1997) 159.
[16] K. Scott, W. Taama, J. Cruickshank, J. Appl. Electrochem. 28 (1998) 289.
[17] H. Dohle, J. Divisek, R. Jung, J. Power Sources 86 (2000) 469.
[18] J.-T. Wang, R.F. Savinell, Proceedings of the Electrochem. Soc. 326, 94–23.
[19] P. Argyropoulos, K. Scott, A.K. Shukla, C. Jackson, J. Power Sources 123 (2003) 190.
[20] A. Kulikovsky, Electrochem. Commun. 5 (2003) 530.
[21] K.T. Jeng, C.W. Chen, J. Power Sources 112 (2003) 367.
[22] A. Havránek, K. Klafki, K. Wippermann, in: Proceedings of the First European Polymer Electrolyte Fuel Cell Forum, Luzern, Switzerland, 2–6 July, 2001, p. 221.
[23] H. Dohle, J. Divisek, J. Mergel, H.F. Oetjen, C. Zingler, D. Stolten, J. Power Sources 105 (2002) 274.
[24] F.N. Buechi, A. Marek, G.G. Scherer, Ext. Abstract of the Electrochem. Soc. 94-1 (1994) 980.
[25] X. Ren, W. Henderson, S.J. Gottesfeld, Electrochem. Soc. 144 (1997) 267.
[26] J. Meyers, J. Newman, J. Electrochem. Soc. 149 (2002) A718.
[27] J. Kim, S.M. Lee, S. Srinivasan, C.E. Chamberlin, J. Electrochem. Soc. 142 (1995) 2670.
[28] H. Dohle, A.A. Kornyshev, A.A. Kulikovsky, J. Mergel, D. Stolten, Electrochem. Comm. 3 (2001) 73.
[29] H. Dohle, Ph.D. Thesis, RWTH Aachen (2000).
[30] P.S. Kauranen, E. Skou, J. Electroanal. Chem. 408 (1996) 189.